Palaeogeography, Palaeoclimatology, Palaeoecology 558 (2020) 109938

Contents lists available at ScienceDirect

Palaeogeography, Palaeoclimatology, Palaeoecology

journal homepage: www.elsevier.com/locate/palaeo

Mortality curves and population structures of late early Miocene Rhinocerotidae (Mammalia, Perissodactyla) remains from the Béon 1 locality of Montréal-du-Gers, France

Manon Hullot*, Pierre-Olivier Antoine

Institut des Sciences de l'Évolution, UMR5554, Université de Montpellier, CNRS, IRD, EPHE, Place Eugène Bataillon, CC064, 34095 Montpellier, France

ARTICLE INFO

Keywords:
Life table
Tooth wear
Age estimate
Taphonomy
Protocol

ABSTRACT

Mortality curves are a valuable tool to study taphonomy and to infer population structure in ancient communities; however, they rely on the precise determination of ontogenetic ages of individual animals, which is often uncertain for fragmentary and isolated fossil remains. In this paper, we develop a new protocol to construct mortality curves for fossil rhinocerotids using both tooth rows and isolated teeth, based on dental wear. We tested and calibrated this protocol using 29 skulls and 18 jaws of extant rhinoceroses (*Diceros bicornis*, *Rhinoceros sondaicus*, and *R. unicornis*). We then applied it to four extinct rhinocerotid species from the late early Miocene locality of Béon 1 of Montréal-du-Gers, SW France: the teleoceratines *Brachypotherium brachypus* and *Prosantorhinus douvillei*, the basal rhinocerotine *Plesiaceratherium mirallesi*, and the early elasmotheriine *Hispanotherium beonense*. Findings allow us to estimate population structures of these rhinocerotids, based on the percentage of juveniles, subadults and adults. The mortality curves of Béon 1 rhinocerotids reveal several major periods of vulnerability: birth, weaning, sexual maturity, and middle-late adulthood. When compared to extant populations (*D. bicornis*, *Ceratotherium simum*, and *R. unicornis*) and other ancient case studies (Miocene of USA, Pleistocene of Southeast Asia and France), mortality rate curves from Béon 1 are similar in early and late life; however, they lack the increased socially-driven mortality that is observed between 25 and 50% of the potential lifespan in some populations of *D. bicornis* and in the Miocene teleoceratine *Teleoceras proterum*. The population structures of *Pr. douvillei*, *Pl. mirallesi,* and *H. beonense* are close to those of extant populations of *D. bicornis*. In contrast, adult specimens of *B. brachypus* are overrepresented at Béon 1, similarly to *Aphelops malacorhinus* at Love Bone Bed (USA), probably due to taphonomical bias. It is important to note that considering isolated or associated teeth alone results in significant differences in mortality curves and population structures at Béon 1, hence both samples should be studied.

1. Introduction

Mortality curves, i.e., graphs showing the number of individuals from a population dying at each age category, are often used for estimating population age structure, proposing attritional causes such as diseases, predation, climate, or post-mortem transport (Fernandez and Legendre, 2003; Bacon et al., 2018), and interpreting life trait histories of given species in archaeological and palaeontological assemblages. They can be compared to living population structures in the wild, which in turn allows for inferring some social aspects of the life of past populations, such as hunting behaviour of humans (Stiner, 1990), or intragender competition (Mihlbachler, 2003) and sexual dimorphism (Mihlbachler, 2007) in rhinoceroses. However, the establishment of such mortality profiles rests on reliable estimates of individual age, which proves to be quite challenging for fossil material, especially when documenting extinct species (Mihlbachler, 2003; Böhmer et al., 2016). As far as extinct mammals are concerned, most studies have based age estimates on teeth due to their abundance and completeness in the fossil record. Parameters of interest include crown height, timing of eruption, cementochronology, and/or tooth wear (Kurtén, 1953; Morris, 1972; Spinage, 1973; Fernandez, 2009).

An extensive bibliography is available for age determination in mammals and especially in hoofed mammals (cervids: Mitchell, 1963; Gilbert, 1966; bovids: Spinage, 1971; Klevezal and Pucek, 1987; equids: Muylle et al., 1996; Guadelli, 1998; Fernandez and Legendre, 2003). To our knowledge, only three studies linking tooth wear and individual age are available in extant rhinoceros species (Goddard, 1970; Hitchins, 1978; Hillman-Smith et al., 1986). Another analysis, focused on the

* Corresponding author.
E-mail addresses: manon.hullot@umontpellier.fr (M. Hullot), pierre-olivier.antoine@umontpellier.fr (P.-O. Antoine).

https://doi.org/10.1016/j.palaeo.2020.109938
Received 4 May 2020; Received in revised form 23 July 2020; Accepted 23 July 2020
Available online 29 July 2020
0031-0182/

Pleistocene *Stephanorhinus hemitoechus*, uses wear to define age groups (Louget, 2006). Seminal works on extant rhinoceros species are focused on the black rhinoceros, *Diceros bicornis* (Goddard, 1970; Hitchins, 1978) and on the white rhinoceros, *Ceratotherium simum* (Hillman-Smith et al., 1986). The first study (Goddard, 1970) defines 20 very short age categories (about a year-long for most of them) but is somehow arbitrary in linking wear and individual age, which the author admits himself. The study of Hitchins (1978) is very complete and combines dental wear and sequence of eruption with counts of annular cementum growth increments (actual age). However, to provide individual age, this protocol is based on (semi-) complete tooth rows and is not adapted to isolated teeth, that makes age estimates more complex and less reliable in most practical cases (Mihlbachler, 2003; Bacon et al., 2015). Indeed, in many fossil-yielding localities, rhinocerotid teeth are found isolated, either due to transport underwater, natural decay of bones, or scavengers (e.g., in Pleistocene caves; Bacon et al., 2015; Fourvel et al., 2015). To study age structure of alleged rhinocerotids from such localities, one of us (POA) has developed a protocol for building mortality curves including isolated teeth, based on the work of Hillman-Smith et al. (1986) that was used in several studies (Bacon et al., 2008, 2015, 2018; Fourvel et al., 2015) but never detailed extensively thus far. Hillman-Smith et al. (1986) define a scale of wear for white rhinoceros teeth and provide a correspondence between the wear stage of every tooth and individual age ranges, leading to the characterisation of 16 age classes based on wear, with a cementum-lines count for each of them.

Here, we i) propose a detailed version of such protocol, ii) complete its proof of concept on other species of living rhinoceroses with known individual ages, iii) apply it to the plurispecific late early Miocene rhinocerotid assemblage of Béon 1 at Montréal-du-Gers (Southwestern France), and iv) compare the corresponding age structures to living and fossil rhinocerotid species and assemblages, with inferences on taphonomy and sociality.

2. Localities studied

2.1. Béon 1, Montréal-du-Gers (late early Miocene)

The fossil locality of Béon 1 was discovered in a limestone quarry in 1987, near the village of Montréal-du-Gers in the Aquitaine Basin (43° 5′ 11.116“N – 0° 13’ 19.606”E, altitude: 144 m; Crouzel et al., 1988). Initially known as “Montréal-du-Gers”, the site was renamed to Béon 1 after the discovery of a second locality about 150 m away from the first one in 1994 (Antoine and Duranthon, 1997; Bulot et al., 2009). Assigned to the late early Miocene mid-Orleanian land mammal age (MN4, ca 17 Mya), Béon 1 has yielded a rich and diverse vertebrate assemblage, the components of which were described in the last decades and including among others artiodactyls, perissodactyls, rodents, lagomorphs, amphibians, proboscideans, carnivorans, squamates, and birds (Crouzel et al., 1988; de Bruijn et al., 1992; Duranthon et al., 1995; Antoine and Duranthon, 1997; Rage and Bailòn, 2005; Orliac, 2006; Orliac et al., 2006). Within this fauna, rhinocerotids widely dominate over other large and middle-sized mammals in terms of abundance (both regarding specimen and individual numbers). Five co-occurring rhinocerotid species have been recognized at Béon 1 (Antoine and Duranthon, 1997; Antoine et al., 2000; Antoine, 2002): the teleoceratines *Brachypotherium brachypus* and *Prosantorhinus douvillei* (hereunder abbreviated *Pr. douvillei*), the rhinocerotines *Plesiaceratherium mirallesi* (hereunder abbreviated *Pl. mirallesi*) and *Plesiaceratherium* sp. (no dental remains), and the elasmotheriine *Hispanotherium beonense*. The inferred environment of Béon 1 is primarily paludal or swamp-like with variations of the water level (Duranthon et al., 1999). Depositional history includes nine phases pointing to a relatively short stratigraphic interval, after subaerial weathering and karstification of underlying lacustrine limestones: 1) deposition of coarse reworked limestone pebbles and silty clays with broken fossils, of fluvial origin, 2) a drying episode leading to the formation of a shallowing oxbow lake, 3) first trampling phase by large vertebrates all over the lake, turning it into a swamp, 4) deposition of dark fossil-rich laminated clays (and sub-connected fossils) in this swamp, 5) second trampling phase by large vertebrates in several areas of the swamp, 6) deposition of grey and oxidized clays with sparse fossils, 7) consolidation, 8) pedogenesis, and 9) deposition of a second lacustrine limestone at the top of the sequence (completed from Duranthon et al., 1999).

From bottom to top, three fossiliferous levels are recognized (Duranthon et al., 1999):

- an irregular surface of karstic limestone on the top of which lay bones packed in coarse sediments, mostly fragmentary and with preferential orientation of the long bones (fluvial origin);
- a 15–50 cm-thick layer of brown very rich in fossils of various dimensions, often in sub-anatomical connection and trampled, and corresponding to oxbow lake-swamp deposits;
- a layer of light-coloured lacustrine marls and clays, with less fossil remains.

2.2. Other localities

2.2.1. Recent populations

Population structures of recent rhinoceroses used in section 6.3 derive from direct observations reported in Pienaar (1994) for *Ceratotherium simum* at Kyle National Park (Zimbabwe: S-20° 10′ 59.997“S – 31° 0’ 59.999”E) and Umfolozi Game Reserve (South Africa: 28° 2′ 24.003“S – 32° 3’ 36.004”E), Laurie et al. (1983) for *Rhinoceros unicornis* at Chitwan National Park (Nepal: 27° 29′ 45.924“N – 84° 24’ 48.427”E), and from Mundy (1984) for *Diceros bicornis* at Hluhluwe-Umfolozi Game Reserve. The mortality rate curves of extant *D. bicornis* were built using data from Goddard (1970) at Tsavo National Park (Kenya: 2° 41′ 43.34“S – 38° 9’ 55.445”E) and Hitchins (1978) in Zululand reserves (South Africa: Hluhluwe-Umfolozi, Mkuze [27° 38′ 32.9”S – 32° 9′ 7.7″E] and Ndumu [26° 53′1.3”S – 32° 15′ 5.6″E] Game Reserves). Both studies were made during several consecutive years, in referencing every dead specimen in the reserves.

2.2.2. Fossil sites

We also considered fossil localities and specimens described elsewhere for comparison. We used the mortality rate curves of rhinocerotids from late Miocene localities of Florida (USA) as established by Mihlbachler (2003), yielding the hornless rhinocerotid *Aphelops malacorhinus* and the short-legged teleoceratine *Teleoceras proterum* at Love Bone Bed (fluvial channel, 9.5–9.0 Ma; Mihlbachler, 2003), as well as *Teleoceras proterum* at Mixson's Bone Bed (lacustrine setting, 9.0–8.0 Ma; Prothero, 2005).

Age structures available in the literature for other fossil rhinocerotids were also added. They encompass Middle and Late Pleistocene taxa from South Asian and French localities, further documenting contrasted climatic, environmental, taphonomic, and taxonomic contexts (Bacon et al., 2008, 2011, 2015, 2018; Antoine, 2012; Fourvel et al., 2015). All data about these localities are summed up in Table 1.

3. Materials

3.1. Abbreviations

In this paper we use the following abbreviations: Anatomical abbreviations: Capital letters are used for the upper teeth (I, incisor; D, deciduous molar; P, premolar; M, molar), while lower case letters indicate lower teeth (i, d, p, m). Institutional abbreviations: MCL, Musée des Confluences, Lyon; MNHN, Muséum National d'Histoire Naturelle, Paris; MHNT, Muséum de Toulouse; UM, Université de Montpellier.

Table 1
Information on the fossil localities included in this paper.

	Description	Location	Age	Rhinocerotid taxa	Use in this study	References
Nam Lot	Cave, karstic site (not in situ deposits)	Northeast Laos (Huà Pan province) 20°42′4”N, 104°27′58″E	86–72 ka	*Rhinoceros sondaicus* *Rhinoceros unicornis* *Rhinoceros* sp. Rhinocerotidae indet	Age structure	Bacon et al. 2012, 2015
Tam Hang	Rockshelter, karstic site (not in situ deposits)	Northeast Laos (Huà Pan province) 20°10′18”N, 103°26′5″E	98–60 ka	*Rhinoceros sondaicus* *Rhinoceros unicornis* *Rhinoceros* sp. Rhinocerotina indet	Age structure	Bacon et al., 2008, 2011
Coc Muoi	Cave	Northeast Vietnam (Lang Son province) 22°21′22”N, 106°26′6″E	148–117 ka	*Rhinoceros sondaicus* *Rhinoceros unicornis* *Dicerorhinus sumatrensis*	Age structure	Bacon et al., 2018
Duoi U'Oi	Cave, karstic site (not in situ deposits)	North Vietnam (Hoà Binh province) 20°37′12”N, 105°16′25″E	66 ± 3 ka (Late Pleistocene)	*Rhinoceros sondaicus* *Rhinoceros unicornis* *Dicerorhinus sumatrensis* *Rhinoceros* sp. Rhinocerotina indet	Age structure	Bacon et al., 2008, 2015
Punung	Cave, karstic site	East Java 8°8′31”S, 111°1′58″E	128–118 ka	*Rhinoceros sondaicus* *Dicerorhinus sumatrensis*	Age structure	Bacon et al., 2015
Sibrambang and Lida Ajer	Cave, karstic site	West Sumatra (Padang Highlands) ~ 4°S, ~104°E	80–60 ka	*Rhinoceros sondaicus* *Dicerorhinus sumatrensis*	Age structure	Bacon et al., 2015
Fouvent-Saint-Andoche (also named Abri Cuvier)	Hyena den and karstic context	Northeast France (Haute-Saône) ~ 47°39′14”N, ~5°40′29″E	Late Pleistocene (Würmian stage)	*Coelodonta antiquitatis*	Age structure	Fourvel et al., 2015
Love Bone Bed	Fluvial system	Florida, USA (Alachua County) 29°32′46”N, 82°31′21”W	Late Miocene (latest Clarendonian)	*Teleoceras proterum* *Aphelops malacorhinus*	Age structure Mortality rate curve	Mihlbachler, 2003
Mixson's Bone Bed	Large sinkole, pondlike environment	Florida, USA (Alachua County) 29°24′ 54”N, 82°25′49”W	Late Miocene (Hemphillian)	*Teleoceras proterum* *Aphelops malacorhinus*	Age structure Mortality rate curve	Mihlbachler, 2003

3.2. Recent material

Material of recent rhinoceroses used for the calibration of this protocol consists of 29 skulls and 18 jaws, belonging to *D. bicornis* (16 skulls, 14 jaws), *Rhinoceros sondaicus* (six skulls, two jaws), and *R. unicornis* (seven skulls, two jaws). They are stored in the collections of the MNHN, of the MCL, and of the UM. Details about these specimens (geographic origin, date of collection, sex, and age) are provided in the supplementary data if available. As extant rhinoceros material is scarce in European collections and individual age rarely available for wild animals, zoo specimens were included in this study (four *D. bicornis* and two *R. unicornis*).

3.3. Fossil material

The dental material of rhinoceros from Béon 1 studied here consists of 50 skulls and 56 jaws with complete and sub-complete tooth rows, and 367 isolated cheek teeth distributed as follows: five jaws (with 28 teeth) and 29 isolated teeth of *B. brachypus*, four skulls, three jaws (totalling 45 teeth), and 66 isolated teeth for *H. beonense*, 23 skulls, 26 jaws (with 238 teeth), and 138 isolated teeth for *Pr. douvillei*, and 23 skulls, 22 jaws (231 teeth), and 134 isolated teeth for *Pl. mirallesi*. The total number of teeth included in the present study is 909, 542 teeth from tooth rows and 367 isolated teeth. Very few teeth from tooth rows could not be used for the protocol because of their bad preservation (e.g., badly broken or occlusal surface not visible): two for *B. brachypus*, one for *H. beonense*, and six for *Pr. douvillei*.

The material from Béon 1 is permanently stored at the MHNT. It was collected through annual excavations led by F. Duranthon, Y. Laurent, and one of us (POA) since 1987.

4. Methods

4.1. Protocol description

In this article we propose, develop, and test a new protocol to estimate individual age based on rhinocerotid dental remains – both isolated and from tooth rows – refining the seminal protocol of Hillman-Smith et al. (1986). A preliminary version by one of us (POA) had previously been applied to Pleistocene samples from Southeast Asia (Bacon et al., 2008, 2015, 2018) and France (Fourvel et al., 2015), encompassing close relatives of extant rhinoceroses and including isolated teeth only. This protocol is primarily based on the study of Hillman-Smith et al. (1986), in which the authors define a scale of dental wear scores based on individuals of *C. simum*, ranging from 1 to 10, 1 standing for unerupted tooth under bone and 10 for worn tooth with no enamel left (Fig. 1). This wear score of every upper and lower jugal tooth (D1-D4, P2–P4 and M1–M3, d1-d4, p2–p4 and m1–m3, respectively) is then linked to the individual age observed in tooth rows of animals with known ages. Hillman-Smith et al. (1986) based their results on 74 individuals, among which nine individuals with exact age were used to estimate the age of 65 other ones. As a result, 16 age classes (I to XVI) were defined, ranging from 0 (new born) to 40-years old (maximum potential lifespan). Nevertheless, in order to avoid considering that maximum potential lifespans are identical in extinct rhinoceroses and in the white rhinoceros, we used preferentially percentage of potential lifespan (Mihlbachler, 2003), age classes (I to XVI), and ontogenetic stages (juvenile, subadult, and adult) instead of numeric individual ages.

We consider here that triangular teeth located in front of P2/p2 are persistent D1/d1, respectively. They are likely to be shed during lifetime in living and fossil rhinocerotid species (Antoine, 2002; Böhmer

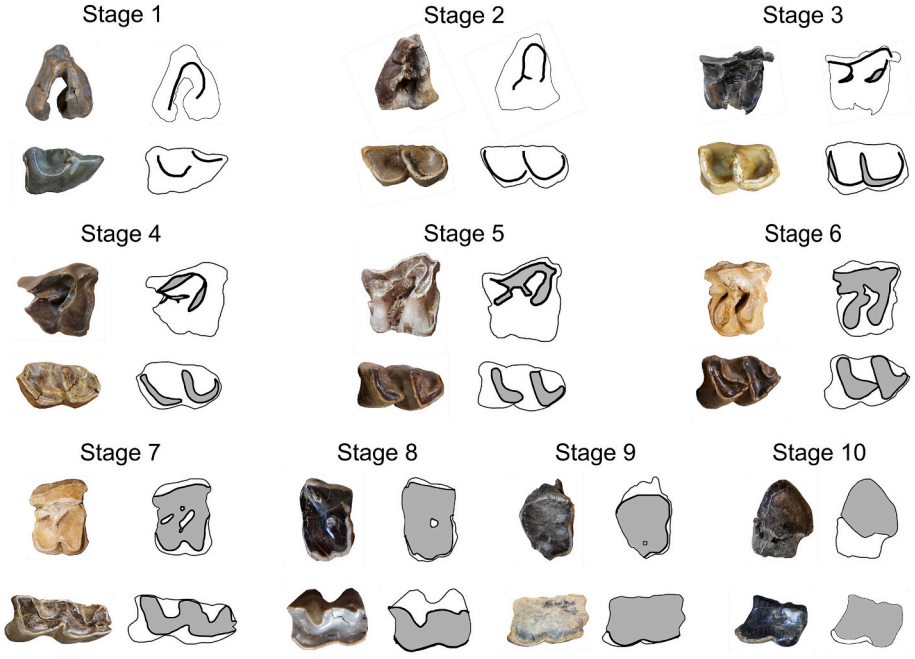

Fig. 1. Examples of upper and lower teeth of fossil rhinocerotids from Béon 1 (late early Miocene, SW France) for every wear score (1 − 10) following the definition of Hillman-Smith et al. (1986). Increasing stages of wear are illustrated with photographs and associated interpretative drawings. Not to scale: all teeth were put at the same size to facilitate the comparisons between the different stages.
Stage 1 – wear score 1: – upper: M3 of *Prosantorhinus douvillei* MHNT.PAL.2015.0.1220, lower: d2 of *Plesiaceratherium mirallesi* MHNT.PAL.2015.0.1206; Stage 2 – wear score 2: upper: M3 of *Pr. douvillei* MHNT.PAL.2015.0.1212 (mirrored), lower: m1 of *Pr. douvillei* MHNT.PAL.2015.0.2826; Stage 3 – wear score 3: upper: D4 of *Pr. douvillei* MHNT.PAL.2015.0.2795, lower: d4 of *Pr. douvillei* MHNT.PAL.2015.0.1708; Stage 4 – wear score 4: upper: M2 of *Pr. douvillei* MHNT.PAL.2015.0.1221 (mirrored), lower: m1 of *Pr. douvillei* MHNT.PAL.2015.0.1248 (mirrored); Stage 5 – wear score 5: upper: M2 of *Hispanotherium beonense* MHNT.PAL.2004.0.58, lower: m3 of *H. beonense* MHNT.PAL.2015.0.1141; Stage 6 – wear score 6: upper: P4 of *Pl. mirallesi* MHNT.PAL.2015.0.1435, lower: m1 of *H. beonense* MHNT.PAL.2015.0.1141; Stage 7 – wear score 7: upper: P4 of *Pl. mirallesi* MHNT.PAL.2015.0.1435 (mirrored), lower: d3 of *Pr. douvillei* MHNT.PAL.2015.0.2826; Stage 8 – wear score 8: upper: P2 *H. beonense* MHNT.PAL.2015.0.1124, lower: m1 of *Pr. douvillei* MHNT.PAL.2015.0.2758 (mirrored); Stage 9 – wear score 9: upper: D1 of *H. beonense* MHNT.PAL.2015.0.1124, lower: m1 of *Pl. mirallesi* MHNT.PAL.2015.0.1186 (mirrored); Stage 10 – wear score 10: upper: D1 of *H. beonense* MHNT.PAL.2015.0.1124, lower: p4 of *H. beonense* MHNT.PAL.2015.0.1134.

et al., 2016). As *C. simum* individuals do not retain persistent D1/d1, no data were available for these teeth in Hillman-Smith et al. (1986), whereas they may persist in all other extant rhinocerotid species and in most fossil taxa (Antoine, 2002).

Thus, we used 10 skulls and eight jaws of *D. bicornis*, five skulls and one jaw of *R. unicornis*, and seven skulls and one jaw of *R. sondaicus* presenting d1/D1 to complete the dataset of Hillman-Smith et al. (1986) on extant rhinoceroses (list of specimens provided in S1). We estimated the probable age class of every of these specimens by observing all other teeth, and scored the wear of the d1/D1 independently. Then, we proposed a range of wear score for d1/D1 corresponding to each age class. At last, we added new columns for persistent d1/D1 in the table provided by Hillman-Smith et al. (1986) accordingly (Table 2).

To estimate the individual age of rhinocerotid specimens, we start by giving every tooth an equal weight (weight [W] = 1), whether it is an isolated tooth or it belongs to a tooth row. Then, we score from 1 to 10 the wear stage of all teeth according to the scale defined by Hillman-Smith et al. (1986) and illustrated in Fig. 1. For each tooth, we eventually propose an age class or a range of age classes as defined by Hillman-Smith et al. (1986), by reporting in Table 2 the score of wear estimated for the tooth and selecting all matching classes. For instance, if a M3 has a wear score of 5, the only age class corresponding to this wear is XIII (Table 2) and the weight assigned to this class XIII is therefore 1. Contrastingly, if a p2 has a wear score of 6, five successive age classes match this wear (VIII-XII; Table 2). As we cannot assign the tooth to any of them with certainty, we consider all these five age classes as being equally plausible, and assign a weight of 1/5 to each ($W_{tooth} = 5 \times 1/5 = 1$).

4.2. Calibration of the protocol

4.2.1. Testing the protocol on extant non-Ceratotherium rhinoceroses with known ages

Based on the results of previous studies (Anderson, 1966; Hitchins, 1978; Fortelius, 1985; Hillman-Smith et al., 1986; Böhmer et al., 2016) and personal observations, we assume that wear-estimated ages are comparable between *Ceratotherium* and most fossil rhinocerotids as their dental pattern and eruption sequence are highly similar. Nevertheless, as an intermediate step, we tested the protocol described hereabove on extant non-*Ceratotherium* rhinoceroses with age constraints. Few specimens with exact age were available in museum collections as labels are often incomplete (Scott et al., 2012) but we could test the protocol on four zoo specimens: three specimens of *D. bicornis* and one of *R. unicornis*. Our protocol gave age intervals consistent with the museum label. However, the span of the interval was sometimes very wide and thus imprecise (see S2). We also found small discrepancies between upper and lower tooth rows intervals, but very rarely between left and right sides. These differences could be somewhat explained by asynchronous eruption between upper and lower (Bigalke et al., 1950; Dittrich, 1972) and by the more variable wear observed on lower tooth rows (Table 2). Indeed, some teeth provide short intervals, as their wear evolves drastically between age classes (e.g., P2 or M3), whereas other display more variable states of wear within similar classes (e.g., lower teeth). In this respect, the protocol of Hitchins (1978) is seemingly better, although subjective and primarily applicable only on complete tooth rows.

4.2.2. Comparison with Hitchins' (1978) protocol

We tested our protocol on five other *D. bicornis* specimens and compared the results for all eight *D. bicornis* specimens to Hitchins' (1978) protocol (S3). Again, we obtained very long age intervals with our protocol, but fully matching the range obtained with Hitchins' (1978) one. We also studied Béon 1 specimens following the latter protocol and confronted that to our results (S4). Age class attributions were quite subjective especially concerning isolated teeth because state description of some teeth is lacking for some classes (for instance class VI only mentions M2, P2/p2 descriptions are absent from class XII). However, when all teeth were considered we obtained similar age distribution profiles for all four species and no significant differences were found between both protocols (Kolmogorov-Smirnov, p-values > 0.05; see S4). All this suggests that our protocol gives less precise, wider age intervals for complete tooth rows but is both more robust in terms of reproducibility and less subjective.

Table 2
Relation between wear score and individual age in upper and lower teeth (permanent and decidual) of living rhinocerotids. The values in the columns for persistent d1/D1, lacking in the original table by Hillman-Smith et al. (1986), were either extrapolated from adjacent values (in bold) or added from personal observation (in grey) on dental series of extant *Diceros bicornis* (the most closely related living rhinoceros; 10 skulls, five jaws), *Rhinoceros unicornis* (five skulls, one jaw), and *Rhinoceros sondaicus* (seven skulls, one jaw). Maximum age (40 years) stands for 100% of potential lifetime. Modified from Hillman-Smith et al. (1986).

Age Category	Assigned ages	Age in% of longevity	Maxilla											Mandible										
			Deciduous teeth					Permanent premolars			Permanent molars			Deciduous teeth					Permanent premolars			Permanent molars		
			Dl (non-persistent)	**Dl** (persistent)	D2	D3	D4	P2	P3	P4	**Ml**	M2	M3	dl (non-persistent)	dl (persistent)	d2	d3	d4	p2	p3	p4	**ml**	m2	m3
0	0-1.5 months	0-0.3	0	0	0	0	0	0	0	0	0	0	0	0	0	0	0	0	0	0	0	0	0	0
I	1.5-2 months	0.3-0.4	0	0	1/2	1/2	0	0	0	0	0	0	0	0	0	1/2	1/2	1/2	0	0	0	0	0	0
II	2-4 months	0.4-0.8	0/1	0/1	2/3	2/3	1/2	0	0	0	0	0	0	0/1	0/1	2/3	2/3	2/3	0	0	0	0	0	0
III	4-12 months	0.8-2.5	1/2	1/2	3/4	3/4	2/3	0	0	0	0	0	0	1/2	1/2	3/4	3/4	2/4	0	0	0	0	0	0
IV	12-18 months	2.5-3.8	3/4	3/4	4/5	4/5	2/3	0	0	0	0/1	0	0	2/3	2/3	4/5	4/5	3/4	0	0	0	0	0	0
V	1.5-3 years	3.8-7.5	7/8	**5/8**	6/7	5/6	4/5	0	0	0	1/2	0	0	8	2/9	6	6	4/5	0	0	0	2	0	0
VI	3-4 years	7.5-10	8/9	**5/9**	7/8	6/7	5/6	0/2	0	0	2/3	0/1	0	8/10	**2/9**	8/9	7/8	6/9	0/1	0/1	0/1	2/3	1	0
VII	3.5-4 years	8.8-10	-/9	**5/9**	8/9	7/8	6/7	2/3	0/1	0	4/5	1	0	9/0	4/10	8/9	8/-	7/8	1/3	1	0	4/5	0/1	0
VIII	4-7 years	10-17.5	-/9	**5/9**	-/9	-/8	7/8	3/4	1/2	1	4/5	2/3	0	9/0	**3/9**	9/-	8/-	7/8	3/8	1/7	1/7	4/6	2/5	1/2
IX	7-9 years	17.5-22.5		**5/9**			-	5/6	4/6	1/2	5/6	3/4	1	9/0	**3/9**	9/-	9/-	9/-	4/7	5/7	3/7	5/7	3/7	1/3
X	8-11 years	20-27.5		6/9			8/9	7/8	6/7	2/3	6	4/5	1		3/9				6/7	6/7	3/7	5/9	3/7	1/4
XI	10-15 years	25-37.5		6/8			8/9	8	6/7	3/5	6/7	4/5	2		7/8				5/8	6/8	4/7	5/8	4/6	2/4
XII	14-20 years	35-50		7/9			-	8/9	7/8	6/7	7/8	5/6	2/3		8/10				6/8	7/8	5/7	6/8	5/6	1/4
XIII	20-28 years	50-70		8/9				-/8	8	8	7/8	6/7	4/6		**9/10**			-	7/10	7/9	7/8	6/10	5/8	4/5
XIV	25-32 years	62.5-80		**9/10**				-	/9	8/9	8	8	7	6	**9/10**			-	7/10	8/9	7/8	7/10	**6/9**	**5/6**
XV	30-38 years	75-95		10					-	8/9	9	8	7/8		10/-				8/10	8/9	8/10	8/10	7/10	6/7
XVI	35-40 years	87.5-100									-	9/10	9							8	-/10	10	8/10	7/8

In bold = interpolation based on surrounding values
In grey= values added by the authors based on personnal observations

4.3. Estimating minimum number of individuals (MNI)

The minimum number of indiviudals (MNI) is usually calculated for a given species on the count of the most abundant anatomical element (e.g. bones or teeth) from the same side (for instance, MNI = 30 in a sample composed of 20 left p2s and 30 right p2s). However, when considering teeth, MNI can be refined according to sequences of tooth eruption, as several teeth are never functional simultaneously. Literature (Anderson, 1966; Hitchins, 1978; Fortelius, 1985; Hillman-Smith et al., 1986; Böhmer et al., 2016) and personal observation give the following sequence for the rhinocerotids, with potentially slight variations depending on the species: (d2/D2, d3/D3), (d1/D1, d4/D4), m1/M1, p2/P2, p3/P3, (m2/M2, p4/P4), m3/M3 (parentheses stand for simultaneous eruption). All milk molars, except from persistent d1/D1, are thus incompatible with functional fourth premolars and third molars, but also with their permanent counterpart (e.g., p2/P2 with d2/D2). Accordingly, we considered four incompatible groups as follows: a) deciduous teeth (excluding d1/D1) and all third molars, b) deciduous teeth (excluding d1/D1) and all fourth premolars, c) d2/D2 and corresponding p2/P2, and d) d3/D3 and corresponding p3/P3. We then determined MNIs for all species within each incompatibility group by adding the two highest numbers of incompatible functional teeth (excluding germs). For instance, MNI as defined on group i) in *Pl. mirallesi* is 22, corresponding to the sum of seven right d3s and 15 right m3s. Finally, we selected the highest MNI of the four incompatibility groups as defining the MNI of the concerned species at Béon 1.

4.4. Construction of age distribution and mortality rate curves

In order to get the age distribution among the sixteen age classes (see section 4.1), we summed all the weights for each class from the teeth falling in it, either fully (W = 1) or partly (W = 1/N, where N is the number of age classes compatible with the wear stage of this tooth). Based on these sums, which do not correspond to a real number of specimens or of individuals, we estimated age structure. Age structure is given through the percentage of specimens in each ontogenetic stage: juveniles, subadults, and adults (see detailed example for all *B. brachypus* teeth in S5). These stages rely on the ages associated with the classes proposed by Hillman-Smith et al. (1986) on living individuals of *Ceratotherium simum* and that were correlated to life events (weaning, sexual maturity) accordingly, albeit not directly observable on fossil specimens. Juveniles comprise individuals in age classes I to V, corresponding to the period from birth to weaning / eruption of the first permanent tooth (m1/M1). Subadults comprise individuals in age classes VI to VIII, which correlates with the period in between weaning / eruption of first permanent tooth and sexual maturity / eruption of last permanent tooth (m3/M3). Eventually, adults include all individuals falling in age classes IX to XVI, from sexual maturity to death / eruption of last permanent tooth (m3/M3).

Mortality rates (q_x) were calculated using the following equation: $q_x = \frac{d_x \times 1000}{i \times l_x}$, where i is the duration of the age class considered (in years), d_x the number of deaths out of 1000 individuals in the same age class, and l_x is the number of survivors in the same age class again.

All statistics were done using R (R Core Team, 2018) and they are detailed in supplementary item S6. Figures were made using R (with ggplot2 and ggtern packages), GIMP (2.8), and Inkscape (0.91).

5. Results

5.1. Minimum numbers of individuals (MNI) by species at Béon 1

We estimated the MNIs on the basis of available dental material and incompatibilities deduced from the sequence of eruption of Rhinocerotidae. We recorded the number of every tooth for the four rhinocerotid species of Béon 1 documented by teeth, and show the results for the teeth in the four incompatibility groups defined in section

4.3 (Table 3). Before considering dental incompatibilities, we estimated a MNI of 17 (based on the number of right P4) for *Pl. mirallesi,* 19 (based on the number of left M2) for *Pr. douvillei*, five for *B. brachypus* (based on right p4) and six for *H. beonense* (based on left m1). Within each incompatibility group we summed the maxima (Table 4) and obtained the following MNIs: five for *B. brachypus*, six for *H. beonense*, 26 for *Pr. douvillei*, and 24 for *Pl. mirallesi* (total = 61). The MNIs of all four rhinocerotid species at Béon 1 were given by the same incompatibility group: group b, corresponding to deciduous teeth (excluding d1/D1) and all fourth premolars (Table 4). The number of individuals within the four species is drastically distinct, *Pl. mirallesi* and *Pr. douvillei* being widely and equally dominant at Béon 1, whereas *B. brachypus* and *H. beonense* are equally scarce.

5.2. Application of the protocol on Béon 1 rhinocerotids (Montréal-du-Gers, France)

First, we applied the protocol described above (section 4.1) to all the teeth (isolated and from tooth rows) of four species of rhinocerotids from Béon 1: the teleoceratines *Brachypotherium brachypus* and *Prosantorhinus douvillei*, the hornless rhinocerotine *Plesiaceratherium mirallesi*, and the early elasmotheriine *Hispanotherium beonense*. The distribution among age classes is shown in Fig. 2. The graph of age distribution, with all species merged (Fig. 2-A) shows three peaks, which suggests that deaths might have affected potentially vulnerable individuals during major biological, physiological, and behavioural events. The peaks observed correspond to juveniles around weaning period (classes V-VI = 3.75 to 10% lifespan [1.5 to 4 years old]), subadults near sexual maturity (classes IX-XI = 17.5 to 37.5% lifespan [7 to 15 years old]), and adults (XII-XIII = 35 to 70% lifespan [14 to 28 years old]). The third peak includes ~120 teeth per class (classes XII-XIII), whereas the first two peaks only present ~55 (classes V-VI) and 90 teeth per class (classes IX-XI), respectively. We do not observe overrepresentation of any age class on this graph.

When species are discretised (Fig. 2-B), the curves obtained are significantly distinct from the curve of merged age distribution curve (Kolmogorov-Smirnov, *p*-values < 0.05; see S6). The number of teeth varies drastically depending on the species considered: *Pl. mirallesi* and *Pr. douvillei* are widely prevailing over *B. brachypus* and *H. beonense* in terms of contribution to the merged age distribution curve. With respect to other species, *B. brachypus* presents an underrepresentation of juveniles (Fig. 2-B), with only one milk tooth in the studied sample (a right D1 – likely to be persistent, though) and no teeth falling in the first three age classes. The first age class is also undocumented for *H. beonense* but juveniles are otherwise well represented proportionally. All curves but that of *Pr. douvillei* have a similar aspect compared to the merged age distribution with the same age class peaking (V-VI, IX-XI, and XII-XIII), although limited in *B. brachypus* (due to the low number of juveniles) and shifted towards class XIII only for *H. beonense*. Concerning *Pr. douvillei* the age distribution exhibits only two peaks, the second being longer and encompassing age classes IX to XIII (Fig. 2). We have also considered separately age distributions as inferred by isolated teeth only on one hand, and by “associated teeth” (from tooth rows), on the other hand (Fig. 3A-D). Except for *Pr. douvillei* (isolated and associated teeth) and *B. brachypus* (associated teeth), the same age classes V-VI, IX-XI, and XII-XIII are peaking. There are twice as much associated teeth as isolated teeth in all species but *B. brachypus*, documented by a similar number of isolated (29) and associated teeth (26). The underrepresentation of juveniles in *B. brachypus* is even more accentuated when considering associated teeth only, as the first seven age classes but the fifth are not documented (Fig. 3A). Both subsamples, isolated and associated, show significant differences from the merged sample depending on the species. There are only differences between all teeth merged and isolated subsample for *Pr. douvillei* (Kolmogorov-Smirnov, p-value = 0.004) and *Pl. mirallesi* (Kolmogorov-Smirnov, *p*-values = 0.01), whereas it is between all teeth merged and associated subsample for *H. beonense* (Kolmogorov-Smirnov, p-value = 0.004). Surprisingly, we did not find significant differences between isolated and associated subsets in any species (Kolmogorov-Smirnov, p-values > 0.05; see S6).

5.3. Impact of unequal and overlapping classes

Age classes as defined by Hillman-Smith et al. (1986) or by Hitchins (1978) are unequal in duration and overlapping, which may blur the interpretation of age distributions. In this section, we built histograms with a weighting step (count in each class divided by class' duration) to assess the impact of such classes (Fig. 4). All corrected curves are strikingly similar between all species from Béon 1, with two modes (one around the juvenile-subadult transition [classes IV-VII], and one in young adults [classes IX-X]), and a distribution of adults more balanced and characterised by a regular decrease towards the last age class (class XVI). The smoother peaks in *B. brachypus* may primarily relate to the low number of teeth and individuals in the available sample. *Plesiaceratherium mirallesi* and *Pr. douvillei* further share a high neonatal peak (classes I-II), lacking in both *H. beonense* and *B. brachypus* maybe because of smaller samples.

5.4. Mortality rate curves (q_x) and population structure of the rhinocerotids from Béon 1

We then constructed mortality rate curves (q_x) based on the life tables (

S7) for the four rhinocerotid species from Béon 1 previously mentioned (Fig. 5A-E). All q_x curves from Béon 1 rhinocerotids are relatively similar, with several peaks in the early life (i.e., before 25% of the lifespan), a plateau between 30 and 75% of the lifespan, and a major peak after 80% of the lifespan. Only, the q_x curve of *H. beonense* is significantly different from that of all other three species (Kolmogorov-Smirnov, p-values < 0.05; see

S6). The curves of *Pr. douvillei* and *Pl. mirallesi* (Fig. 5D-E) display similarly high q_x, around 25, at the beginning of the life that is not found in the other two species. Besides this early peak, the curves of *Pl. mirallesi* and *H. beonense* are very similar, in intensity and shape of the peaks at around 3, 9, and 20% of the lifespan (Fig. 5C, E). The peak around 3% of lifespan is much attenuated in the curves of the two teleoceratines (Fig. 5B, D) but the other two peaks (i.e., 9 and 20% of lifespan) are present with a different shape.

At last, we estimated population structure with the percentages of teeth within each ontogenetic stage – juvenile, subadult, adult – for every rhinocerotid species from Béon 1 (S8). We plotted the results in a ternary diagram (Fig. 6) for all teeth merged, isolated teeth only, and associated teeth (i.e., belonging to tooth rows) only. For all species but *B. brachypus*, there are as many juveniles as subadults and a majority of adults. For all teeth merged, *Pr. douvillei* and *H. beonense* display similar age structures with about 15% of juveniles, 17% of subadults, and 68% of adults. *Plesiaceratherium mirallesi* presents a slightly different structure with less juveniles (~13%) and subadults (~12%) but more adults (~75%). Here again, *B. brachypus* has an underrepresentation of juveniles (less than 3%), but about the same percentage of subabults (~11%) as *Pl. mirallesi*.

Except for *H. beonense*, discrepancies exist between age structures estimated from isolated and associated teeth (Fig. 6). When present, they are all illustrating a shift towards adult stage, either strong (~25% in *Pr. douvillei*) or moderate (~12% in *Pl. mirallesi* and ~ 15% in *B. brachypus*), when only associated teeth are taken into account. Variation for *H. beonense* is minor, with slightly more subadults and less juveniles and adults inferred from associated teeth.

6. Discussion

In this paper we focused on rhinocerotid species from Béon 1

Table 3
Number of rhinocerotid teeth by dental locus and species at Béon 1, excluding germs (i.e., unerrupted unworn teeth).

	D2				D3				D4			
	Upper		Lower		Upper		Lower		Upper		Lower	
	Left	Right	Left	Right	Left	Right	Left	Right	Left	Right	Left	Right
Incompatibility group	a, b, c	a, b, c	a, b, c	a, b, c	a, b, d	a, b, d	a, b, d	a, b, d	a, b	a, b	a, b	a, b
B. brachypus	0	0	0	0	0	0	0	0	0	0	0	0
H. beonense	2	3	2	2	3	3	1	1	1	1	0	3
P. douvillei	3	3	2	3	3	9	3	3	6	7	6	5
P. mirallesi	7	4	4	2	5	1	4	7	4	1	7	3

	P2				P3				P4				M3			
	Upper		Lower		Upper		Lower		Upper		Lower		Upper		Lower	
	Left	Right	Left	Right	Left	Right	Left	Right	Left	Right	Left	Right	Left	Right	Left	Right
Incompatibility group	c	c	c	c	d	d	d	d	b	b	b	b	a	a	a	a
B. brachypus	0	2	1	0	3	4	0	0	4	5	1	0	3	4	1	1
H. beonense	3	3	1	1	2	2	2	2	2	3	1	3	3	2	2	3
P. douvillei	3	8	8	8	6	13	9	6	7	12	10	17	6	12	14	12
P. mirallesi	8	10	7	11	10	5	14	14	15	8	16	17	9	8	13	15

Incompatibility groups are based on dental eruption sequence, as some teeth are never functional at the same time. Group a: deciduous teeth (excluding d1/D1) and all third molars; Group b: deciduous teeth (excluding d1/D1) and all fourth premolars; Group c: d2/D2 and corresponding p2/P2; Group d: d3/D3 and corresponding p3/P3.

Table 4
Minimum number of rhinocerotid individuals (MNI) estimated in the four groups of incompatibility by species at Béon 1.

	B. brachypus	*H. beonense*	*P. douvillei*	*P. mirallesi*
MNI group a	4	6	23	22
MNI group b	5	6	26	24
MNI group c	2	6	11	15
MNI group d	4	5	22	21
MNI total	5	6	26	24

Incompatibility groups are based on dental eruption sequence, as some teeth are never functional at the same time. Group a: deciduous teeth (excluding d1/D1) and all third molars; Group b: deciduous teeth (excluding d1/D1) and all fourth premolars; Group c: d2/D2 and corresponding p2/P2; Group d: d3/D3 and corresponding p3/P3.
Group b provides the highest MNI for each species.

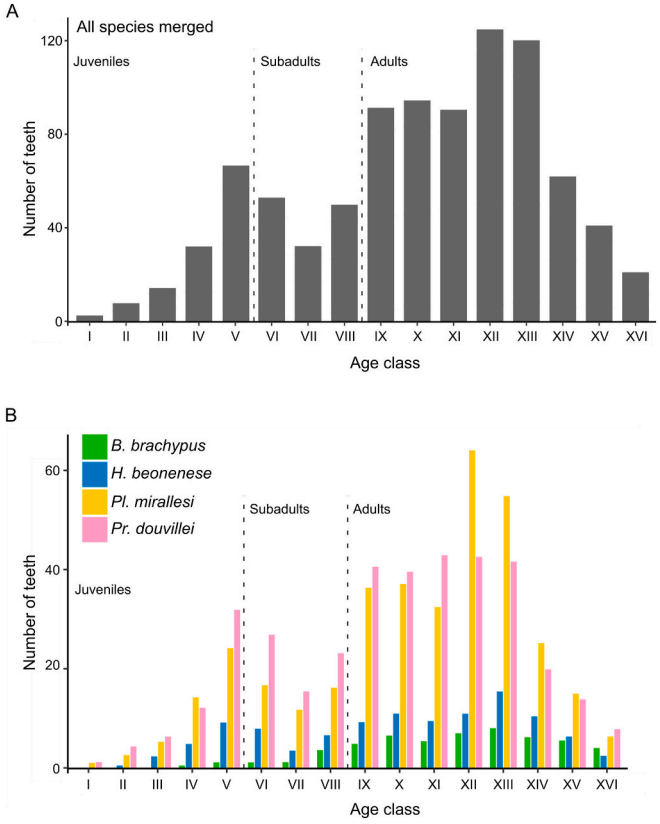

Fig. 2. Mortality curves of rhinocerotid teeth from Béon 1 (late early Miocene; SW France). A- All species merged, B- Species considered separately: *Brachypotherium brachypus* in green, *Hispanotherium beonense* in blue, *Plesiaceratherium mirallesi* in yellow, and *Prosantorhinus douvillei* in pink. Age classes from I to XVI based on dental wear as defined by Hillman-Smith et al. (1986). (For interpretation of the references to colour in this figure legend, the reader is referred to the web version of this article.)

because of their exceptional abundance and their good representation among age classes, from unworn milk molars to very worn third permanent molars.

6.1. Minimum numbers of individuals (MNI) estimates: Teeth vs. postcranials

Despite our adjustment based on incompatibility groups (Table 4), teeth-based MNIs are underestimated with respect to those assessed with other indicators. For instance, astragalus-based MNIs for the most abundant species at Béon 1, *Pr. douvillei* and *Pl. mirallesi*, are 40 and 38 respectively versus 26 and 24 using teeth. In contrast, the astragalus-based MNI for *H. beonense* is seven, instead of six using teeth. This low discrepancy confirms that MNIs do exaggerate the relative abundance of rare species in a given assemblage, as already concluded by Plug and Plug (1990). Postcranial data are not sufficient at Béon 1 for comparing teeth (MNI = 6) and astragali in *B. brachypus*. In any event, this would suggest a more accurate MNI of 91 rhinocerotids at Béon 1, instead of 61 based on teeth only, which demonstrates the interest of taking into account any available data for evaluating MNIs, including postcranial remains.

6.2. Age distribution and mortality: Biases and social implications

The mortality curves of rhinocerotid teeth from Béon 1 (Fig. 2, Fig. 3, Fig. 4) suggest several vulnerability periods depending on the species. The first period, identified as the neonatal period (classes I-II), observed on corrected age distributions (Fig. 4), is found in *Pl. mirallesi* and *Pr. douvillei* only. Contrastingly, all rhinocerotid species from Béon 1 exhibit a vulnerability period corresponding to juveniles around weaning period (classes IV-VII = 2.5 to 10% lifespan [1 to 4 years old]). This is known to be a critical time for extant rhinoceros calves because they become independent before adult size is reached (Owen-Smith, 1988), leading to higher predation susceptibility (Brain et al., 1999) and food stress (Mead, 1999). Another period of vulnerability is found near the hypothesised sexual maturity (classes IX-XI = 17.5 to 37.5% lifespan [7 to 15 years old]). This could be explained through the prism of behaviour and sociality of rhinoceroses. Indeed, the courtship and mating is violent in some living rhinoceros species, whether it be male fights for dominance, male rejection by the female, female chasing by males or mating wounds (Owen-Smith, 1988; Zecchini, 1998; Dinerstein, 2003). Eventually, the last period of vulnerability occurs in middle to late adulthood (XII-XIII = 35 to 70% lifespan [14 to 28 years old]) but this is attenuated in the corrected curves (Fig. 4). An increase mortality late in life is not surprising, and could be due to several parameters such as senility, diseases, or advanced dental wear leading to feeding difficulties. In the extant *R. unicornis*, this is also a period when bulls over 20 years old display solitary behaviour (Laurie et al., 1983; Bacon et al., 2018). Although it would have been enlightening about some social aspects, we were not able to identify sex for enough specimens to analyse intersex differences in Béon 1 rhinocerotids, as it could be proposed for *Menoceras arikarense* at Agate Springs (Mihlbachler, 2007): our sample is composed of many isolated teeth and very few tooth rows present obvious dimorphic signs (e.g., incisors in situ, distinct mandibular robustness, or diverging mandibular angles). On another hand, further work is underway on the prevalence of hypoplasia (i.e., indicator of physiological stress) and patterns of dental microwear (i.e., indicator of diet) of Béon 1 rhinocerotids, which might shed light on potential causes to these vulnerability periods (Hullot et al., work in progress).

6.3. Mortality rate (q_x) and population structure at Béon 1: comparison to extant populations and other fossil samples

In stable populations, mortality profiles are U- or L-shaped as deaths are more frequent among the youngest and oldest members of a population (Mihlbachler, 2003). The mortality rate curves from Béon 1 (Fig. 5B-E) are quite close to these idealised attritional mortality profiles. Indeed, when juveniles are well represented such as for *Pl. mirallesi* and *Pr. douvillei*, we observe a high mortality in the early life (Fig. 4; Fig. 5D-E). However, they display age-specific mortality rates with several peaks in early life (before 25% of lifespan). We compared Béon 1 q_x curves to those of two extant black rhinoceros populations (Fig. 5F-G) and to those of three fossil samples (Fig. 5H-J). The q_x curves of *H. beonense* and *Pl. mirallesi* are very similar to that of *D. bicornis* from Zululand reserves (Hitchins, 1978). However, all q_x curves

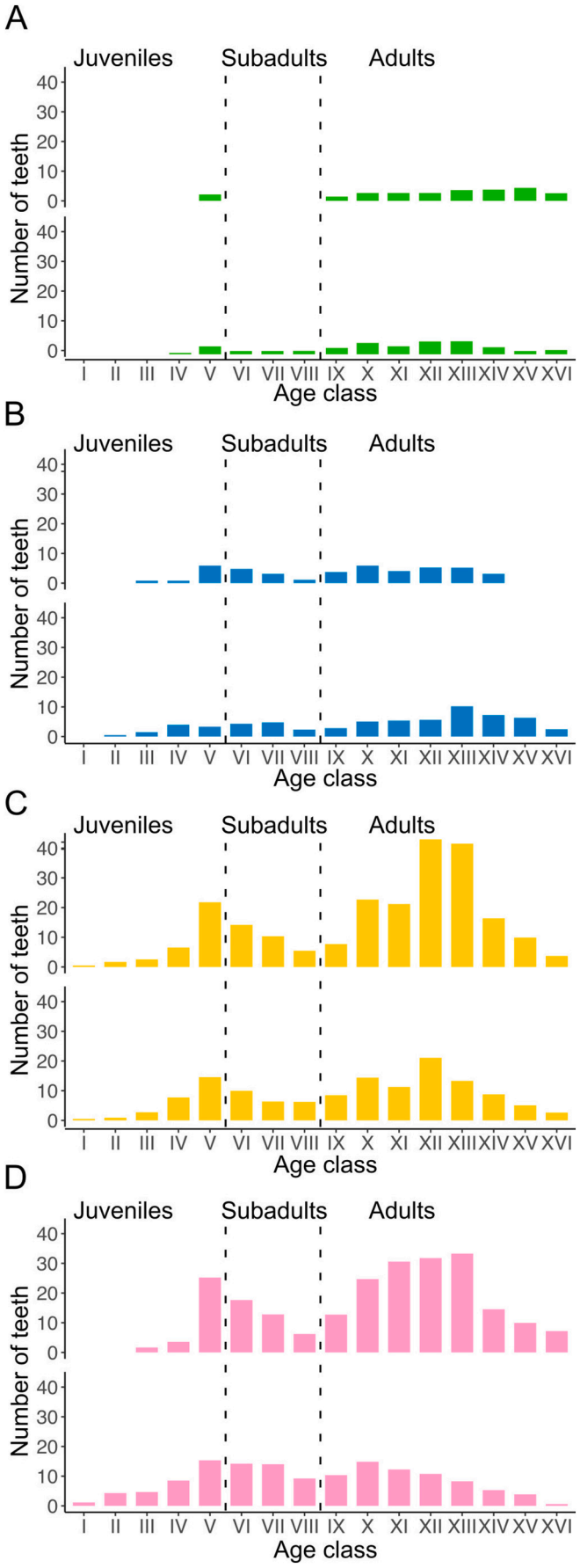

Fig. 3. Comparative mortality curves as documented by associated (upper curves) and isolated (lower curves) teeth of rhinocerotids from Béon 1, late early Miocene, SW France.
A- *Brachypotherium brachypus,* B- *Hispanotherium beonense*, C- *Plesiaceratherium mirallesi*, D- *Prosantorhinus douvillei*. Associated teeth (top curves for each panel) are those belonging to complete or semi-complete tooth rows. Colour code same as in Fig. 2 (green, *B. brachypus*, blue; *H. beonense*; yellow, *Pl. mirallesi*; pink, *Pr. douvillei*). Age classes from I to XVI based on dental wear as defined by Hillman-Smith et al. (1986). (For interpretation of the references to colour in this figure legend, the reader is referred to the web version of this article.)

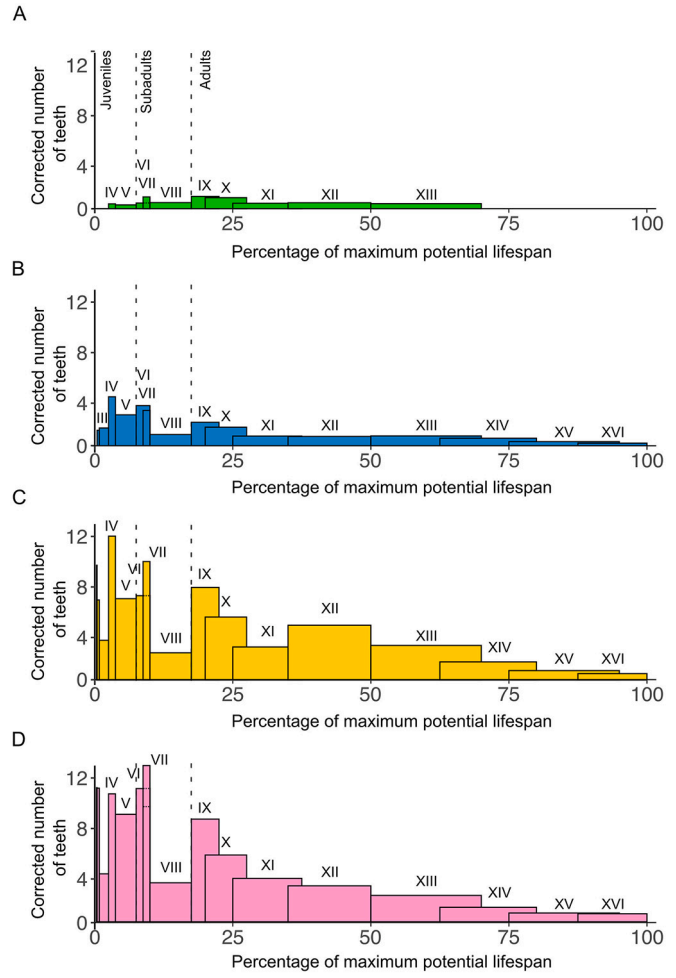

Fig. 4. Corrected age distributions of Béon 1 rhinocerotids, using Hillman-Smith et al.'s (1986) age classes interpreted in terms of potential lifespan percentages. Specimen counts were divided by the duration of the corresponding age class to obtain histograms. Notice duration discrepancies and partial overlaps between some adjacent classes. A- *Brachypotherium brachypus,* B- *Hispanotherium beonense*, C- *Plesiaceratherium mirallesi*, D- *Prosantorhinus douvillei*. Colour code same as in Fig. 2 (green, *B. brachypus*, blue; *H. beonense*; yellow, *Pl. mirallesi*; pink, *Pr. douvillei*). (For interpretation of the references to colour in this figure legend, the reader is referred to the web version of this article.)

from Béon 1 are different from that of *D. bicornis* from Tsavo (Goddard, 1970), those of *Teleoceras proterum* (from both Love Bone Bed and Mixson's Bone Bed) and that of *Aphelops malacorhinus* (Mihlbachler, 2003). This suggests that Béon 1 rhinocerotids did not exhibit high-intensity, lethal male fights as found in some *D. bicornis* groups and probably in *T. proterum* but not in other large herbivores such as hippos (*Hippopotamus amphibius*) or moose (*Alces alces*), as discussed by Mihlbachler (2003).

Noteworthy is the discrepancy between population structures inferred on either the complete dental sample, associated teeth, or

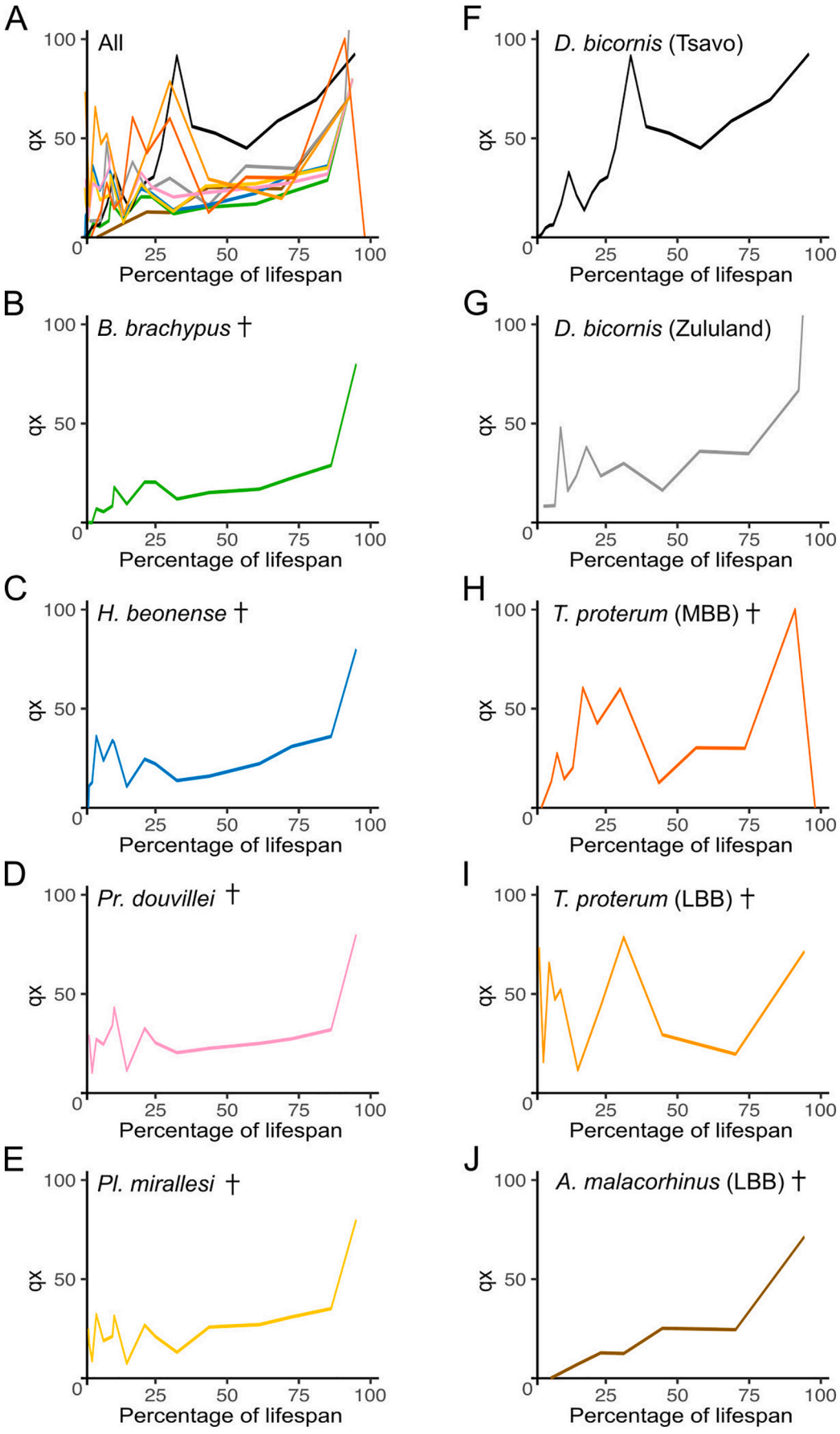

(caption on next page)

Fig. 5. Mortality rate curves (q_x) of various rhinocerotid species, either extant or extinct.
q_x is the mortality rate calculated as the number of mortalities out of a group of 1000 for each percentage of lifespan: $qx = \frac{dx \times 1000}{i \times lx}$ where d_x = deaths per age class, l_x = number of survivors, and i = duration of age class. (†) denotes extinct species. A- All species represented; B to E, q_x of species from Béon 1: B- *Brachypotherium brachypus* (†), C- *Plesiaceratherium mirallesi* (†), D- *Hispanotherium beonense* (†), *E- Prosantorhinus douvillei* (†). F to J, q_x of fossil and extant species adapted from other studies: F- *Diceros bicornis* from Tsavo National Park (Goddard, 1970), G- *Diceros bicornis* from Zululand (Hitchins, 1978), H- *Teleoceras proterum* (†) from Mixson's Bone Bed (Mihlbachler, 2003), I- *Teleoceras proterum* (†) from Love Bone Bed (Mihlbachler, 2003), J- *Aphelops malacorhinus* (†) from Love Bone Bed (Mihlbachler, 2003).

isolated teeth only (Fig. 6). When considering only associated teeth (from skulls and jaws), there is a clear overrepresentation of adults for *Pr. douvillei*, *Pl. mirallesi*, and *B. brachypus* at Béon 1, with respect to isolated teeth (Fig. 6). In the near total absence of predation marks on rhinoceros bones at Béon 1, this bias may be due to preferential decay of the more porous, brittle, and unfused bones in juveniles and subadults than in adults, especially after experiencing post-mortem trampling as observed in the locality (see Subsection 2.1). Interestingly, many historical museum collections host preferably associated teeth (in tooth rows, maxillae, jaws, or skulls), which may in turn lead to similar biases in the inferred mortality curves and/or population structures (i.e., overrepresentation of adults). On the other hand, using only isolated teeth (see Bacon et al., 2008, 2015, 2018; Fourvel et al., 2015) may lead to opposite biases (i.e., underrepresentation of adults). If the best solution consists of considering both associated and isolated teeth in a given locality, one shall be aware of potential biases in alternative study cases.

To characterise the nature of Béon 1 rhinocerotid samples, as based on the complete tooth collection (isolated and associated), we compared them to those of six extant natural rhinoceros populations (Fig. 7A) – two of *C. simum*, three of *D. bicornis*, and one of *R. unicornis* – and to ten fossil samples (Fig. 7B). As for extant rhinoceroses, all species-based samples from Béon 1 coincide with adult-dominated populations. Accordingly, they cluster in the upper third of the ternary diagram (Fig. 7A), as for *A. malacorhinus* and *T. proterum* from Mixson's and Love Bone Beds (Fig. 7B). In terms of structure, the samples of *Pr. douvillei*, *Pl. mirallesi*, and *H. beonense* at Béon 1 fall within the range of natural extant populations, thus suggesting that they are likely to reflect natural population structures, with very minor preservation and taphonomical biases. Furthermore, they are remarkably similar to recent

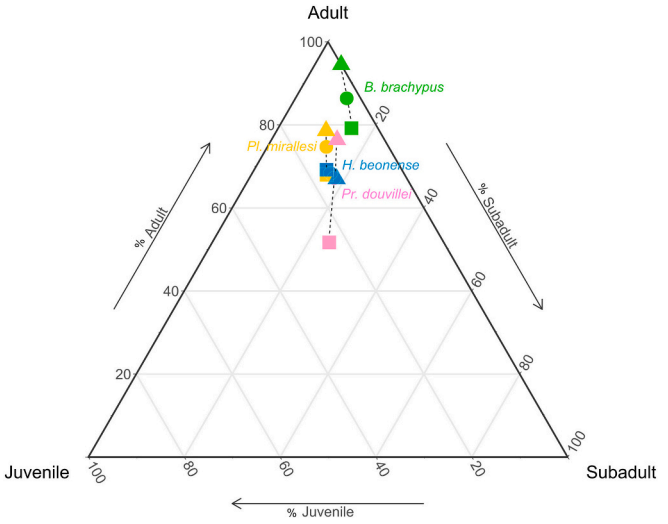

Fig. 6. Population structure of the rhinocerotid species from Béon 1, late early Miocene, SW France. Circles stand for all teeth merged, triangles for associated teeth (i.e., from tooth rows) only, and squares for isolated teeth only. Colour codes as in Fig. 2: green: *Brachypotherium brachypus*, blue: *Hispanotherium beonense*, yellow: *Plesiaceratherium mirallesi*, and pink: *Prosantorhinus douvillei*. Dashed lines link all teeth subsamples within each species (i.e., all, associated, and isolated). (For interpretation of the references to colour in this figure legend, the reader is referred to the web version of this article.)

D. bicornis populations. At Béon 1, the small *B. brachypus*' sample is over-dominated by adults (see subsection 5.2), in a way strikingly comparable to that of *A. malacorhinus* from Love Bone Bed (Fig. 7B) or to *M. arikarense* from Agate Springs (Mihlbachler, 2007). This may point towards similar taphonomical biases in all cases, either due to preservation (i.e., juveniles are more fragile and less likely to get preserved), to spatial origin (i.e., death occurring at different places depending on age; Mihlbachler, 2003), to predation, or to any other unknown reasons. At least at Béon 1, very few tooth marks are found on rhinocerotids (23 remains out of more than 3750 specimens inventoried, i.e. < 0.6%), which makes predation unlikely as a primary bias, especially for *B. brachypus*, which is the largest and heaviest rhinocerotid of the assemblage. Other fossil samples considered in this comparison are Middle to Late Pleistocene in age. Most of them document plurispecific assemblages of extant Asian rhinoceros species from localities in Vietnam, Laos, and Indonesia (*R. unicornis*, *R. sondaicus*, and/or *Dicerorhinus sumatrensis*). The last sample, from Fouvent-Saint-Andoche, France, is assigned to the woolly rhinoceros (*Coelodonta antiquitatis*, extinct). The corresponding samples are all dominated by juveniles. This distinctive structure, with respect to recent populations and Miocene localities, is mostly related to attritional processes. Indeed, Fouvent-Saint-Andoche has all the characteristics of a hyena den, hence indicating a major predatory bias (Fourvel et al., 2015). Concerning Southeast Asian localities, predation effect are also suggested for Nam Lot (by spotted hyena), Coc Muoi and Sibrambang (by tiger), but scavengers such as porcupines (*Hystrix brachyura*) have played a major role in all sites in carrying most specimens to their den and gnawing them there (Bacon et al., 2018). All fossil sites (including Béon 1 and American sites) form a continuum of "population" structures ranging from around 90% of juveniles to 90% of adults. However, no population/sample, neither extant nor fossil, is dominated by subadults (no site plots in lower left corner of the ternary diagram; Fig. 7). This could be partly explained by our definition of the ontogenic stages based on dental wear and eruption, as male subadults or young immature adults may be very abundant punctually (e.g., *Teleoceras proterum*: Mihlbachler, 2003; white rhinoceros: Owen-Smith, 1988).

6.4. Scope and limits of the protocol

Our protocol was developed based on *C. simum* and a preliminary version has been previously applied to Pleistocene close relatives of extant rhinoceroses documented by isolated teeth only. Here, we extended this protocol to representatives of major suprageneric taxa among Rhinocerotidae (two Miocene teleoceratines and a stem rhinocerotine within Rhinocerotinae; an elasmotheriine within Elasmotheriinae), documented by both associated and isolated teeth. The use of *C. simum* as a primary reference for all rhinocerotids might seem somewhat inappropriate, as this species is a hypergrazer with some dental specificities among extant Rhinocerotina (Hullot et al., 2019), such as plagiolophodont and hypsodont teeth, filled with cement. Nevertheless, this compelling choice was made *faute de mieux*, as no wide-ranging study focussing on dental eruption and macrowear is available in other extant rhinoceroses.

As for every method based on teeth, diet, local environment, and dental Bauplan would affect age estimation, similarly to individual age interfering with diet inferences when using mesowear for instance (Rivals et al., 2007). Another issue is that this protocol, just as many

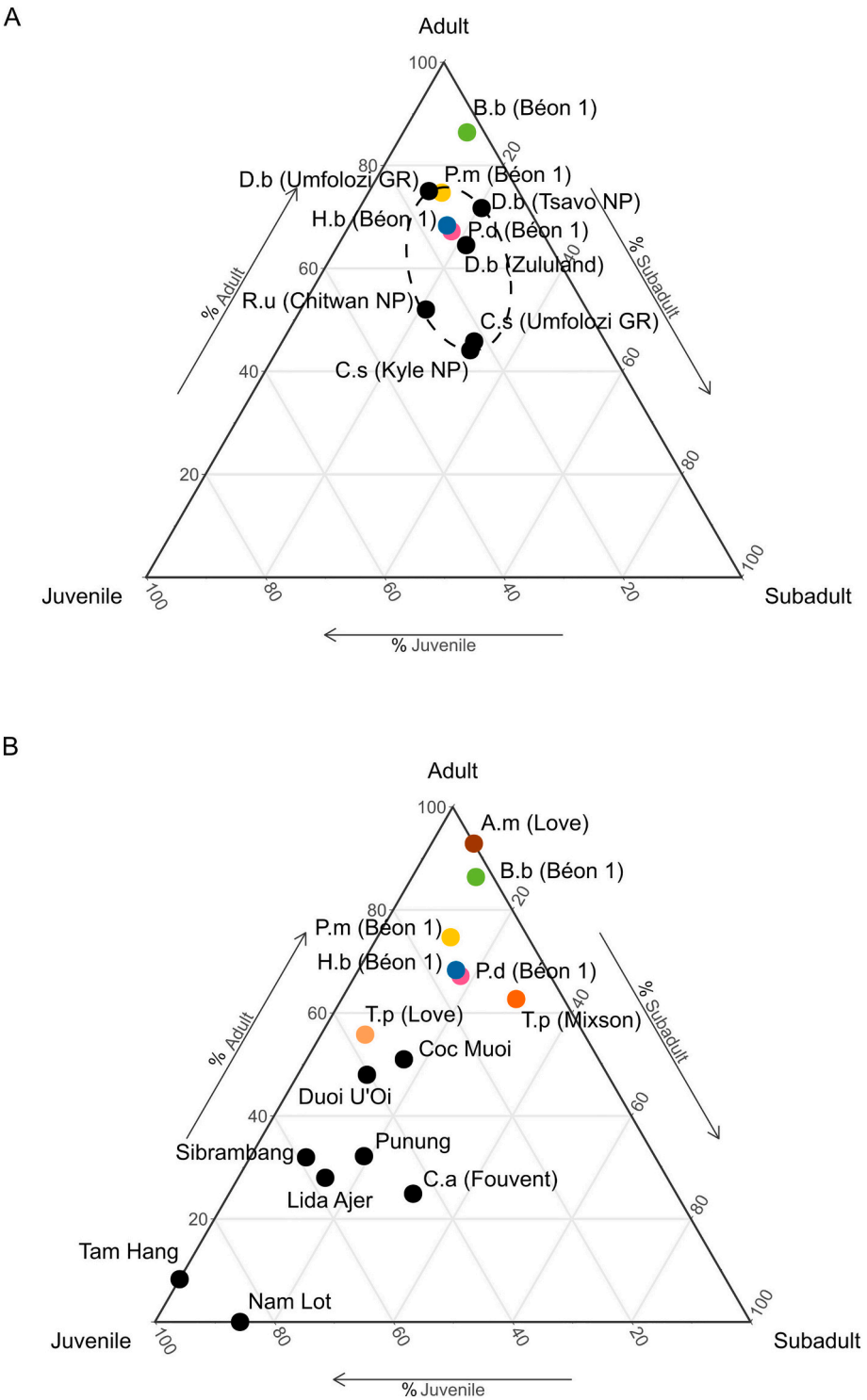

Fig. 7. Population structures of Béon 1 rhinocerotids compared to extant natural populations (A) and other fossil samples (B). Abbreviations: B.b – *Brachypotherium brachypus*, D.b – *Diceros bicornis*, C.s – *Ceratotherium simum*, H.b. – *Hispanotherium beonense*, P.m – *Plesiaceratherium mirallesi*, P.d – *Prosantorhinus douvillei*, A.m – *Aphelops malacorhinus*, T.p – *Teleoceras proterum*, C.a – *Coelodonta antiquitatis*, NP – National Park, GR – game reserve. The grey dashed ellipse represents the range of extant rhinoceros population structures.

other palaeontological studies, relies on an accurate taxonomic and morpho-anatomical identification (which species, which dental locus?). Such an identification can be challenging, especially when it comes to fragmentary or worn teeth. Lastly, scoring the teeth may result in both intra- and inter-observer errors. Both for identification and scoring, we suspect an "observer expertise-based" bias as well. Implementing machine-learning methods for detecting dentine coverage of the tooth could be interesting to lower those biases.

Despite some limits, either intrinsic (e.g., unequal and/or redundant age classes) or extrinsic (e.g., small samples; availability of isolated vs. associated teeth), our protocol proved to be neutral, quite robust in terms of reproducibility, and hopefully accurate for future studies.

7. Conclusions

In the late early Miocene Béon 1 locality, *Pr. douvillei* and *Pl. mirallesi* are equally dominant over two other rhinocerotid species (*B. brachypus* and *H. beonense*), equally scarce. Mortality curves of these four species were built using a new protocol for age estimation in rhinocerotids, based on all available dental remains (associated plus isolated teeth). The age distributions reveal several periods of vulnerability in the life of Béon 1 rhinocerotids depending on the species, likely matching neonatal period, weaning, sexual maturity, and middle-late adulthood. Using only associated or isolated teeth generates a bias in terms of inferred population structure, at least at Béon 1, with substantial overrepresentation and underrepresentation of adults, respectively. It is thus widely preferable to include all available teeth in a given locality. As supported by mortality curves, mortality rate curves, and population structure, most rhinocerotid samples at Béon 1 (*Pr. douvillei*, *Pl. mirallesi*, and *H. beonense*) are likened to extant observed populations, whereas adults and subadults might be overrepresented in *B. brachypus* (based on a small sample, though).

Declaration of Competing Interest

None.

Acknowledgements

We are indebted to Y. Laurent and P. Dalous who gave us access to the collections of the Muséum d'Histoire Naturelle de Toulouse where Béon 1 material is stored. We are also grateful to all the persons in charge of the collections we visited for extant rhinoceroses: S. Jiquel, B. Marandat, and A.-L. Charruault (University of Montpellier), D. Berthet and F. Vigouroux (Musée des Confluences de Lyon), J. Lesur and V. Bouetel (Muséum National d'Histoire Naturelle, Paris). We warmly acknowledge all three reviewers (F. Rivals, M. Mihlbachler, and P. Fernandez), the editor-in-chief (T. Algeo), and the associate editor (H. Falcon-Lang), the comments and inputs of whom greatly improved the manuscript. This work was partly funded by the Fondation Yves Coppens.

Appendix A. Supplementary data

Supplementary data to this article can be found online at https://doi.org/10.1016/j.palaeo.2020.109938.

References

Anderson, J.L., 1966. Tooth replacement and dentition of the black rhinoceros (*Diceros bicornis* Linn.). Lammergeyer 6, 41–46.
Antoine, P.-O., 2002. Phylogénie et évolution des Elasmotheriina (Mammalia, Rhinocerotidae). Mémoires du Muséum national d'Histoire naturelle 188, 5–350.
Antoine, P.-O., 2012. Pleistocene and Holocene rhinocerotids (Mammalia, Perissodactyla) from the Indochinese Peninsula. Comptes Rendus Palevol 11, 159–168.
Antoine, P.-O., Duranthon, F., 1997. Découverte de *Protaceratherium minutum* (Mammalia, Rhinocerotidae) dans le gisement Orléanien (MN 4) de Montréal-du-Gers (Gers). Annales de Paléontologie (Vert.-Invert.) 83, 201–213.
Antoine, P.-O., Bulot, C., Ginsburg, L., 2000. Les rhinocérotidés (Mammalia, Perissodactyla) de l'Orléanien (Miocène inférieur) des bassins de la Garonne et de la Loire: intérêt biostratigraphique. Comptes Rendus de l'Académie des Sciences, Paris 330, 571–576.
Bacon, A.-M., Demeter, F., Tougard, C., de Vos, J., Sayavongkhamdy, T., Antoine, P.-O., Bouasisengpaseuth, B., Sichanthongtip, P., 2008. Redécouverte d'une faune pléistocène dans les remplissages karstiques de Tam Hang au Laos : Premiers résultats. Comptes Rendus Palevol 7, 277–288.
Bacon, A.-M., Duringer, P., Antoine, P.-O., Demeter, F., Shackelford, L., Sayavongkhamdy, T., Sichanthongtip, P., Khamdalavong, P., Nokhamaomphu, S., Sysuphanh, V., Patole-Edoumba, E., Chabaux, F., Pelt, E., 2011. The Middle Pleistocene mammalian fauna from Tam Hang karstic deposit, northern Laos: New data and evolutionary hypothesis. Quat. Int. 245, 315–332.
Bacon, A.-M., Westaway, K., Antoine, P.-O., Duringer, P., Blin, A., Demeter, F., Ponche, J.-L., Zhao, J.-X., Barnes, L.M., Sayavonkhamdy, T., Thuy, N.T.K., Long, V.T., Patole-Edoumba, E., Shackelford, L., 2015. Late Pleistocene mammalian assemblages of Southeast Asia: New dating, mortality profiles and evolution of the predator–prey relationships in an environmental context. Palaeogeogr. Palaeoclimatol. Palaeoecol. 422, 101–127.
Bacon, A.-M., Antoine, P.-O., Huong, N.T.M., Westaway, K., Tuan, N.A., Duringer, P., Zhao, J., Ponche, J.-L., Dung, S.C., Nghia, T.H., Minh, T.T., Son, P.T., Boyon, M., Thuy, N.T.K., Blin, A., Demeter, F., 2018. A rhinocerotid-dominated megafauna at the MIS6-5 transition: the late Middle Pleistocene Coc Muoi assemblage, Lang Son province, Vietnam. Quat. Sci. Rev. 186, 123–141.
Bigalke, R., Steyn, T., de Vos, D., de Waard, K., 1950. Observations on a juvenile female square-lipped or white rhinoceros (*Ceratotherium simum simum* (Burch.)) in the National Zoological Gardens of South Africa. Proc. Zool. Soc. London 120, 519–528.
Böhmer, C., Heissig, K., Rössner, G.E., 2016. Dental Eruption Series and Replacement Pattern in Miocene *Prosantorhinus* (Rhinocerotidae) as Revealed by Macroscopy and X-ray: Implications for Ontogeny and Mortality Profile. J. Mamm. Evol. 23, 265–279.
Brain, C., Forge, O., Erb, P., 1999. Lion predation on black rhinoceros (*Diceros bicornis*) in Etosha National Park. Afr. J. Ecol. 37, 107–109.
de Bruijn, H., Daams, R., Daxner-Höck, G., Fahlbusch, V., Ginsburg, L., Mein, P., Morales, J., Heizmann, E., Mayhew, D.F., Van der Meulen, A.J., Schmidt-Kittler, N., Telles Autunes, M., 1992. Report of the RCMNS working group on fossil mammals, Reisensburg 1990. Newsl. Stratigr. 26, 65–118.
Bulot, C., Antoine, P.-O., Duranthon, F., 2009. Rongeurs et lagomorphes du Miocène inférieur de Béon 2 (MN4, Montréal-du-Gers, SW France). Annales de Paléontologie 95, 197–215.
Crouzel, F., Duranthon, F., Ginsburg, L., 1988. Découverte d'un riche gisement à petits et grands mammifères d'âge Orléanien dans le département du Gers (France). Comptes rendus de l'Académie des sciences. Série 2. Mécanique, Physique, Chimie, Sciences de l'univers, Sciences de la Terre 307, 101–104.
Dinerstein, E. 2003: The return of the Unicorns: the Natural history and Conservation of the Greater One-Horned Rhinoceros. Columbia University Press, p.
Dittrich, L., 1972. Birth and growth of a male White rhinoceros (*Cerathotherium simum simum*) at Hanover Zoo. International Zoo Yearbook 12, 122–125.
Duranthon, F., E. P. J. Heizmann, and P. Tassy. 1995: Safari miocène. Muséum d'Histoire Naturelle de Toulouse:40p.
Duranthon, F., Antoine, P.O., Bulot, C., Capdeville, J.P., 1999. Le Miocène inférieur et moyen continental du bassin d'Aquitaine Livret-guide de l'excursion des Journées Crouzel (10 et 11 juillet 1999). Bulletin de la Société d'histoire naturelle de Toulouse 135, 79–91.
Fernandez, P., 2009. De l'estimation de l'âge individuel dentaire au modèle descriptif des structures d'âge des cohortes fossiles : l'exemple des Equidae et du time-specific model en contextes paléobiologiques pléistocenes. Bulletin de la Société préhistorique française 106, 5–14.
Fernandez, P., Legendre, S., 2003. Mortality curves for horses from the Middle Palaeolithic site of Bau de l'Aubesier (Vaucluse, France): methodological, palaeo-ethnological, and palaeo-ecological approaches. J. Archaeol. Sci. 30, 1577–1598.
Fortelius, M., 1985. Ungulate cheek teeth: developmental, functional, and evolutionary interrelations. Acta Zool. Fenn. 180, 1–76.
Fourvel, J.-B., Fosse, P., Fernandez, P., Antoine, P.-O., 2015. Large mammals of Fouvent-Saint-Andoche (Haute-Saône, France): a glimpse into a late Pleistocene hyena den. Geodiversitas 37, 237–266.
Gilbert, F.F., 1966. Ageing White-tailed deer by annuli in the cementum of the first incisor. J. Wildl. Manag. 30, 200–202.
Goddard, J., 1970. Age criteria and vital statistics of a black rhinoceros population. Afr. J. Ecol. 8, 105–121.
Guadelli, J.-L., 1998. Détermination de l'âge des chevaux fossiles et établissement des classes d'âge/Age determination of fossil horses and the establishment of age classes. Paléo, Revue d'Archéologie Préhistorique 10, 87–93.
Hillman-Smith, A.K.K., Owen-Smith, N.R., Anderson, J.L., Hall-Martin, A.J., Selaladi, J.P., 1986. Age estimation of the white rhinoceros (*Ceratotherium simum*). J. Zool. 210, 355–377.
Hitchins, P. M. 1978: Age determination of the black rhinoceros (*Diceros bicornis* Linn.) in Zululand. South African Journal of Wildlife Research - 24-month delayed open access 8:71–80.
Hullot, M., Antoine, P.-O., Ballatore, M., Merceron, G., 2019. Dental microwear textures and dietary preferences of extant rhinoceroses (Perissodactyla, Mammalia). Mammal Research 64, 397–409.
Klevezal, G.A., Pucek, Z., 1987. Growth layers in tooth cement and dentine of European bison and its hybrids with domestic cattle. Acta Theriol. 32, 115–128.
Kurtén, B., 1953. Age groups in fossil Mammals. Societas Scientiarum Fennica Commentationes Biologicae 13, 1–6.
Laurie, W.A., Lang, E.M., Groves, C.P., 1983. Rhinoceros unicornis. Mamm. Species 211, 1–6.
Louget, S., 2006. Determining the Age of death of Proboscids and Rhinocerotids from Dental Attrition. Pp.179–188. In: Ruscillo, D. (Ed.), Recent Advances in Ageing and Sexing Animal Bones.
Mead, A.J., 1999. Enamel hypoplasia in Miocene rhinoceroses (*Teleoceras*) from Nebraska: evidence of severe physiological stress. J. Vertebr. Paleontol. 19, 391–397.
Mihlbachler, M.C., 2003. Demography of late Miocene rhinoceroses (*Teleoceras proterum* and *Aphelops malacorhinus*) from Florida: linking mortality and sociality in fossil assemblages. Paleobiology 29, 412–428.
Mihlbachler, M.C., 2007. Sexual Dimorphism and Mortality Bias in a Small Miocene north American Rhino, *Menoceras arikarense*: Insights into the Coevolution of Sexual Dimorphism and Sociality in Rhinos. J. Mamm. Evol. 14, 217–238.
Mitchell, B., 1963. Growth layers in dental cement for determining the age of red deer (*Cervus elaphus* L.). J. Anim. Ecol. 36, 279–293.
Morris, P., 1972. A review of mammalian age determination methods. Mammal Rev. 2, 69–104.

Mundy, P.J., 1984. Rhinoceros in South and South West Africa.
Muylle, S., van Loon, G., Simoens, P., Lauwers, H., 1996. Les incisives de cheval : sont-elles vraiment des chronomètres de l'âge? Pratique vétérinaire équine 28, 47–50.
Orliac, M.J., 2006. *Eurolistriodon tenarezensis*, sp. nov., from Montréal-du-Gers (France): implications for the systematics of the European Listriodontinae (Suidae, Mammalia). J. Vertebr. Paleontol. 26, 967–980.
Orliac, M.J., Antoine, P.-O., Duranthon, F., 2006. The Suoidea (Mammalia, Artiodactyla), exclusive of Listriodontinae, from the early Miocene of Béon 1 (Montréal-du-Gers, SW France, MN4). Geodiversitas 28, 685–718.
Owen-Smith, N.R., 1988. Megaherbivores: the Influence of very large Body size on Ecology. Cambridge University Press.
Pienaar, D., 1994. Social organization and behaviour of the white rhinoceros. In: Proceedings of a symposium on "rhinos as game ranch animals.", pp. 87–92.
Plug, C., Plug, I., 1990. MNI counts as estimates of species abundance. The South African Archaeological Bulletin 53–57.
Prothero, D.R., 2005. The Evolution of north American Rhinoceroses. Cambridge University Press.
R Core Team, 2018. A language and environment for statistical computing. R Foundation for Statistical Computing, Vienna, Austria. https://www.R-project.org/.
Rage, J.-C., Bailòn, S., 2005. Amphibians and squamate reptiles from the late early Miocene (MN 4) of Béon 1 (Montréal-du-Gers, southwestern France). Geodiversitas 27, 413–441.
Rivals, F., Mihlbachler, M.C., Solounias, N., 2007. Effect of ontogenetic-age distribution in fossil and modern samples on the interpretation of ungulate paleodiets using the mesowear method. J. Vertebr. Paleontol. 27, 763–767.
Scott, R.S., Teaford, M.F., Ungar, P.S., 2012. Dental microwear texture and anthropoid diets. Am. J. Phys. Anthropol. 147, 551–579.
Spinage, C.A., 1971. Geratodontology and horn growth of the impala (*Aepyceros melampus*). J. Zool. 164, 209–225.
Spinage, C.A., 1973. A review of the age determination of mammals by means of teeth, with especial reference to Africa. Afr. J. Ecol. 11, 165–187.
Stiner, M.C., 1990. The use of mortality patterns in archaeological studies of hominid predatory adaptations. J. Anthropol. Archaeol. 9, 305–351.
Zecchini, A., 1998. Le rhinocéros: au nom de la corne. Editions L'Harmattan 1–272.